Finite-size effects in the static structure factor $S(k)$ and $S(0)$ for a two-dimensional Yukawa liquid

Vitaliy Zhuravlyov * and J. Goree
Department of Physics and Astronomy, University of Iowa, Iowa City, Iowa 52242, USA

Paolo Elvati and Angela Violi
Department of Mechanical Engineering, University of Michigan, Ann Arbor, Michigan 48109, USA

(Received 26 May 2023; accepted 29 August 2023; published 21 September 2023)

Finite-size effects in the static structure factor $S(k)$ are analyzed for an amorphous substance. As the number of particles is reduced, $S(0)$ increases greatly, up to an order of magnitude. Meanwhile, there is a decrease in the height of the first peak S_{peak}. These finite-size effects are modeled accurately by the Binder formula for $S(0)$ and our empirical formula for S_{peak}. Procedures are suggested to correct for finite-size effects in $S(k)$ data and in the hyperuniformity index $H \equiv S(0)/S_{\text{peak}}$. These principles generally apply to $S(k)$ obtained from particle positions in noncrystalline substances. The amorphous substance we simulate is a two-dimensional liquid, with a soft Yukawa interaction modeling a dusty plasma experiment.

DOI: 10.1103/PhysRevE.108.035211

I. INTRODUCTION

The static structure factor $S(k)$ is a function used to describe the arrangement of particles in a substance. Analogous to a diffraction pattern, it characterizes the microscopic structure of the substance. When $S(k)$ is computed from the positions of individual particles, finite-size effects could play a significant role. In this paper we quantify these effects and propose procedures to improve upon them. Our literature search did not reveal recent papers that prominently mention finite-size effects in the $S(k)$ curves obtained from a finite number of particles. Most of the relevant literature [1–14] that we have found is from the 1980s and 1990s, describing finite-size effects for isothermal compressibility χ. That quantity has a theoretical relation to the value of $S(k)$ at $k = 0$, i.e., for infinitely long scale lengths. This relation, for equilibrium conditions, is

$$\chi = S(0)/nk_BT, \tag{1}$$

where n is the particle number density [15–17].

Our focus on finite-size effects for $S(k)$ is motivated by recent interest in the theoretical concept of hyperuniformity [18–33], which refers to a special type of spatial order characterized by the suppression of long-wavelength density fluctuations. For a hyperuniform system, $S(k)$ exhibits a distinctive behavior at small k, i.e., long distances. Specifically, $S(k)$ approaches zero, or becomes strongly suppressed, as $k \to 0$. Hyperuniform substances are predicted to have unique photonic and mechanical properties [22]. As a practical measure of hyperuniformity of a substance, the hyperuniformity index [22,34]

$$H \equiv S(0)/S_{\text{peak}} \tag{2}$$

is the ratio of two values from the $S(k)$ curve: its value at $k = 0$ and the height S_{peak} of the first peak of $S(k)$. These two values and in particular their finite-size effects will be the focus of this paper.

For our finite-size effect analysis, we adopt a notation so that the values for a finite size N are distinguished from the values for an infinite system. Hereafter, we will write $S(k, N)$ as the static structure factor curve obtained using a finite number N of particles and likewise $S(0, N)$ and $S_{\text{peak}}(N)$ as its values at $k = 0$ and at the first peak, respectively. These are distinguished from the values $S(k)$, $S(0)$, and S_{peak} for an infinite system, i.e., as $N \to \infty$.

We briefly summarize how $S(k, N)$ is calculated from positions $\mathbf{r}_i(t)$ of a finite number N of particles. These particles may be physical particles imaged by cameras in experiments [33,35–37] or models of real particles in a numerical simulation [38–41]. This method can be used for liquids as in the present paper, as well as amorphous molecular solids. The instantaneous particle density $\rho(\mathbf{k}, N, t)$ for a finite size N is calculated as

$$\rho(\mathbf{k}, N, t) = \sum_{i=1}^{N} \exp[i\mathbf{k} \cdot \mathbf{r}_i(t)], \tag{3}$$

where k is a specified value of a wave number [15]. Subtracting the average value of $\rho(\mathbf{k}, N, t)$ yields $\tilde{\rho}(\mathbf{k}, N, t)$, which is the input to an autocorrelation calculation

$$S(k, N, t) = N^{-1}\langle \tilde{\rho}(\mathbf{k}, N, t)\tilde{\rho}^{\,*}(\mathbf{k}, N, t)\rangle_\theta, \tag{4}$$

where $\langle\,\rangle_\theta$ is an angular average. Calculations of (3) and (4) can be repeated for not only various values of the magnitude of the wave vector $\mathbf{k}$ but its direction as well. If the available data were not just from a single snapshot of particle positions but were recorded over a range of time, one would perform a time average to obtain the static structure factor

$$S(k, N) = \langle S(k, N, t)\rangle_t. \tag{5}$$

In an initial assessment of the finite-size effects in the static structure factor obtained from particle positions using expressions like Eqs. (3)–(5), Zhuravlyov *et al.* [42] used

* vitaliy-zhuravlyov@uiowa.edu

data from a molecular-dynamics simulation. They reported opposite trends: The calculated value of static structure factor near $k = 0$ decreased, while the height of the first peak increased, with an increasing number of particles N. Those results were for a two-dimensional (2D) liquid, with a Yukawa interparticle interaction to model a dusty plasma with highly charged micron-size particles immersed in an ionized gas.

In this paper, to extend that initial assessment of the finite-size effects, we analyze simulation data over a much wider range of N, up to nearly 10^6 particles. We use these results to test two formulas, by fitting them. The Binder formula [1] is found to accurately model the system-size dependence of $S(k, N)$ at small k, i.e., $S(0, N)$. Likewise, another formula, that we suggest is found to describe how the height of the first peak $S_{\text{peak}}(N)$ depends on N. Furthermore, these results, along with Eq. (2), allow us to assess how the hyperuniformity index H depends on the analyzed system size.

We review the Binder formula along with its historical context in Sec. II, where we also present our empirical formula for the height of the first peak $S_{\text{peak}}(N)$. The 2D Yukawa liquid and simulation method are described in Secs. III and IV, respectively. Particle-position data were used with Eqs. (3)–(5) to calculate $S(k, N)$ for analyzed regions of varying size N, leading to our primary results that are presented in Sec. V. These results lead us to suggest, in Sec. VI, procedures useful for correcting $S(k)$ data for finite-size effects.

II. FORMULAS FOR FINITE-SIZE EFFECTS TO TEST

A. Finite-size effects for $S(k, N)$ at small k

While in this paper we are primarily interested in the finite-size effects of $S(k)$, we must turn to another physical parameter, the isothermal compressibility χ, for historical context. While we found a paucity of literature for finite-size effects in $S(k)$, there is a considerable number of papers [1–14] for finite-size effects in χ. The latter studies motivate our work because they offer practical formulas for finite-size effects and there is a theoretical connection between $S(0)$ and χ in Eq. (1).

The formulas that describe finite-size effects for χ were presented beginning with a paper by Binder [1]. In Binder's notation, the best estimate of the true isothermal compressibility χ for an infinite system is related to the value for a finite system χ_L by

$$\chi_L = \chi - \chi_b L^{-1}, \tag{6}$$

where the factor $\chi_b L^{-1}$ is the finite-size correction for an analyzed region of a linear dimension L. We will refer to Eq. (6) as the Binder formula. Essentially, the Binder formula is an expansion with a single term for a small correction due to finite size.

The history behind the Binder formula traces back to a scaling theory of Fisher and Barber [43]. Their paper was for critical phenomena in a film of finite thickness, which they generalized for various dimensions. Fisher and Barber took into account the boundary conditions of this thin film by using a first-order expansion for a thermodynamic quantity, which was the critical temperature. The paper by Fisher and Barber motivated Landau to investigate finite-size behavior of compressibility along with other thermodynamic parameters, in a 3D Ising lattice [44]. Landau's paper in turn motivated Binder's paper on Ising lattices in various dimensions, and this paper included the formula for susceptibility, which is the same as isothermal compressibility. After Binder's publication, the formula was used by other authors for various physical systems, including binary mixtures [7], polymers [9], hard-disk fluids [11,45], and Lennard-Jones fluids [3,4,6]. Among those who investigated 2D Lennard-Jones fluids were Rovere *et al.* [3], who chose to add a second-order correction to the first-order correction of Binder. To describe trends with varying N, starting with Binder, all the authors we cited used two phrases: finite-size effects and boundary corrections. Many of these authors used the two terms interchangeably and some further complicated their terminology by mixing in a third phrase: boundary effects. For the present paper we will simply use the term finite-size effects.

We will rewrite the Binder formula (6) in terms of not χ and L, but instead $S(0)$ and N. For three dimensions the Binder formula becomes

$$S(0, N) = S(0) + bN^{-1/3}, \tag{7}$$

and for two dimensions it is

$$S(0, N) = S(0) + bN^{-1/2}. \tag{8}$$

Here $S(0) \equiv S(0, N \to \infty)$ is the asymptote for large N. To obtain Eqs. (7) and (8) we combined Eqs. (6) and (1), motivated by the way Eq. (1) theoretically relates two properties of an infinite system, χ and $S(0)$. We converted the L dependence of Eq. (6) to the N dependence of Eqs. (7) and (8) using $L = (N/n)^{1/3}$ and $L = (N/n_{2D})^{1/2}$, for three and two dimensions, respectively, where n_{2D} is the areal number density.

The coefficient b will in general depend on the physical system and its temperature. One can obtain the value of b by fitting data for various values of N, as we will demonstrate later.

For studies of hyperuniformity, the value of $S(0)$ is especially important. For that purpose, we can rewrite Eqs. (7) and (8) with $S(0)$ on the left side, so that for three dimensions we have

$$S(0) = S(0, N) - bN^{-1/3}, \tag{9}$$

while for two dimensions we get

$$S(0) = S(0, N) - bN^{-1/2}. \tag{10}$$

In Eqs. (9) and (10) the last terms are the first-order correction terms. We note that the power law for the correction term obviously depends on the dimensionality of the system. The power law in that correction term is unfortunately weak, meaning that obtaining good precision with a simulation might require an enormously large particle number N, especially in three dimensions with an exponent of only $-1/3$, unless one corrects the simulation result using the Binder formulas, Eq. (9) for three dimensions and Eq. (10) for two dimensions. This correction requires knowledge of the coefficient b, which as we mentioned depends on the substance and its temperature. As a demonstration, we will obtain this coefficient in Sec. V for a 2D Yukawa liquid.

B. Finite-size effects for the first peak of $S(k, N)$

Here we will propose an empirical formula to model finite-size effects for the height of the first peak $S_{\rm peak}(N)$. We found no previous reports of such a formula in our literature search, perhaps because the finite-size effects were studied mostly for another quantity, isothermal compressibility, which is only related to $S(0)$, not $S_{\rm peak}$. We anticipate that other researchers may wish to correct the first peak's height for finite-size effects, for example, in calculating the hyperuniformity index using Eq. (2).

In constructing our empirical formula, we are motivated by the use of a power law in the Binder formula for $S(0, N)$. Thus, we seek an expression for $S_{\rm peak}(N)$ that includes a power law. Moreover, the formula must converge to an asymptotic value as N increases, as in the Binder expression, but with a different trend, since $S_{\rm peak}(N)$ increases instead of decreases with N. A simple formula meeting these requirements is

$$S_{\rm peak}(N) = \frac{S_{\rm peak}}{1 + (N/N_0)^{-\alpha}}. \tag{11}$$

The numerator $S_{\rm peak} \equiv S_{\rm peak}(N \to \infty)$ is the asymptotic value.

The empirical formula (11) has a power-law exponent α and a coefficient $1/N_0$. We consider both of them as free parameters for fitting, for our test of Eq. (11) using data from our 2D Yukawa liquid simulation. Further work would be needed to determine how α and $1/N_0$ depend on other choices of the temperature, density, dimensionality of the physical system, and interparticle potential. Once the exponent α and the coefficient $1/N_0$ are known, the desired quantity $S_{\rm peak}$ can be obtained

$$S_{\rm peak} = S_{\rm peak}(N)[1 + (N/N_0)^{-\alpha}], \tag{12}$$

which is simply Eq. (11) rewritten with $S_{\rm peak}$ on the left side.

III. 2D YUKAWA LIQUID

In this paper we consider a 2D Yukawa liquid. The binary interaction potential for such a system is $(Q^2/4\pi\epsilon_0 r)\exp(-r/\lambda)$, where Q is the particle charge and λ is a screening length for the medium between two particles separated by distance r. One reason for interest in 2D Yukawa liquids is that they model experiments with dusty plasmas.

A dusty plasma is a mixture of solid charged particles and an ionized gas consisting of electrons, ions, and neutral gas atoms [46–49]. In laboratory experiments [50–52], the dust particles are typically of a few microns in size with a negative charge of thousands of elementary charges. The interactions among the dust particles are governed by a screened Coulomb repulsion, which is a soft interparticle interaction that is often modeled as the Yukawa potential [53].

The large charge of the dust particles allows them to be electrically levitated so that they are not in contact with any solid surface [54–56]. When they are levitated in a single horizontal layer [57–64], they can all be imaged using a video camera, which allows the measurement of their positions in each video frame [65]. The large charge also causes the interparticle potential energy of dust particles to be so large that it dominates over their thermal kinetic energy. This condition [66,67], known as strong coupling, leads the particles to self-organize in a crystalline structure [68–71]. Such a crystal can then be melted, using rastered laser beams, to sustain a steady liquid condition [72–74].

In Zhuravlyov *et al.* [42], particle-position data were analyzed for the dusty plasma experiment of Haralson and Goree [75,76], as well as for data from a Yukawa molecular dynamics simulation. The results from the simulation and experiment were found to be consistent, indicating that even though it had simplified physics, the simulation was able to capture the most important aspects of the static structure factor for the experiment. These simulation data were also used in an initial assessment of finite-size effects for measurements of the static structure factor at long wavelengths, i.e., at small k.

In this paper we explore the finite-size effects more comprehensively. The same simulation method was used, as in Ref. [42], but with a much larger system size. Moreover, we also test two formulas for finite-size effects: the Binder formula (8) for $S(0, N)$ and our empirical formula (11) for $S_{\rm peak}(N)$.

IV. SIMULATION

Here we briefly summarize the simulation details. The LAMMPS code [77] was used to perform a molecular-dynamics simulation of identical particles in a microcanonical ensemble. The particles interacted via the Yukawa potential with a cutoff radius of $20a$, where

$$a \equiv (\pi n_{\rm 2D})^{-1/2}$$

is the 2D Wigner-Seitz radius. The dimensionless parameters describing the Yukawa system are the Coulomb coupling parameter Γ and the screening parameter κ defined as in Ref. [42], which were chosen to be 130 and 0.719, respectively. For the corresponding number density, the kinetic temperature had a value that exceeded the melting point T_m for a 2D Yukawa system [78] by a factor of 1.19. The system was equilibrated to the target temperature by a thermostat [79], with the same time constant and integration time step as in the work of Zhuravlyov *et al.* [42], and then the thermostat was turned off. Particle positions were recorded at intervals of $10\omega_0^{-1}$ over a duration of $5000\omega_0^{-1}$, where $\omega_0 \equiv \omega_{pd}/\sqrt{2}$ as in Ref. [42]. Here $\omega_{pd} = (Q^2/2\pi\epsilon_0 M a^3)^{1/2} = 89\ {\rm s}^{-1}$ is a 2D dusty plasma frequency, where M is the particle mass. The boundary conditions for the simulation were periodic. Further details of the simulation method can be found in Ref. [42].

To study the finite-size effects of the static structure factor $S(k, N)$, we varied the size of a circular analyzed region centered within a large simulation box. The simulation box itself was square, containing a fixed number of 937 501 particles, much greater than in Ref. [42]. The analyzed regions were smaller and did not strictly contain a fixed number of particles, as they could leave or enter the region randomly. Hence, we will report time-averaged values of the number N of particles, ranging from $N = 70$ up to $N = 736\,771$, according to the chosen diameter of the circular region analyzed. Example snapshot of particles in some of the smaller analyzed regions is shown in Fig. 1. Data for $S(k, N)$, for the analyzed regions reported in this paper, can be found in Ref. [80].

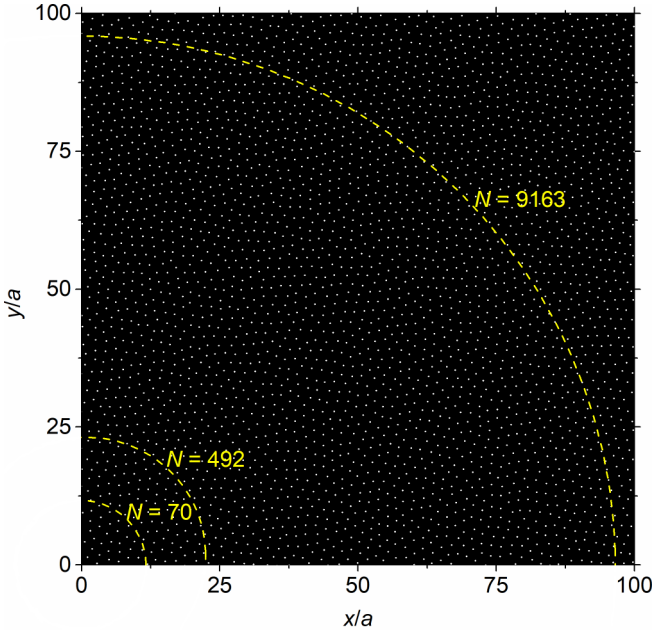

FIG. 1. Tiny portion of the simulation box, showing individual particle coordinates at one time. Also shown are quarters of the three circular regions analyzed, which in total contained on average $N = 70$, 492, and 9163 particles. The entire simulation box, which is too large to show here, is a square containing 937 501 particles, with periodic boundary conditions. Distances are normalized by the 2D Wigner-Seitz radius $a = (\pi n_{2D})^{-1/2}$, for an areal number density n_{2D}. This snapshot reveals the degree of microscopic disorder for this 2D Yukawa liquid, at a temperature above the melting point T_m by a factor of 1.19.

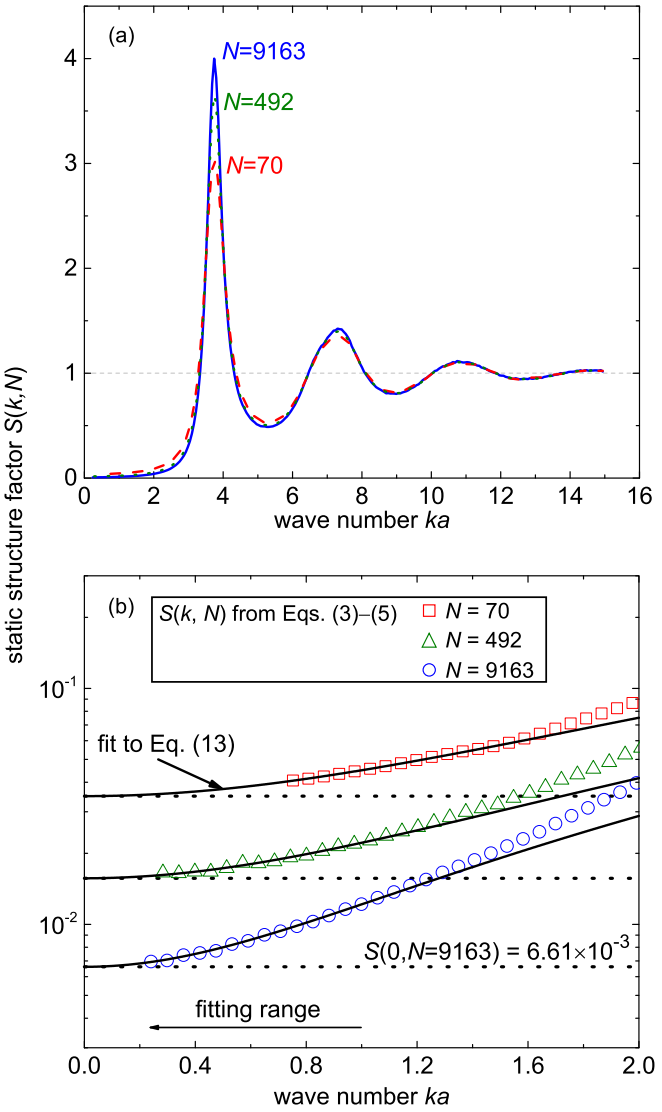

FIG. 2. Static structure factor $S(k, N)$ data. Here the wave number k is normalized by the 2D Wigner-Seitz radius a. The $S(k, N)$ data were obtained using Eqs. (3)–(5) with an input of particle positions from 500 snapshots of the simulation. We varied the size of the analyzed region over 20 values of N, three of which are shown here, as in Fig. 1. The same $S(k, N)$ data are shown as curves in (a) and data points in (b). Semilogarithmic axes in (b) help reveal the finite-size effects at small k. The smooth curves in (b) are parabolas, Eq. (13) obtained by fitting the data points in the range $ka \leqslant 1$. That fit also yielded the extrapolated values of $S(0, N)$ shown as dotted lines.

V. RESULTS

A. Assessing the finite-size effects

We now present the results of our analysis of the 2D Yukawa simulation. The static structure factor $S(k, N)$ curves were obtained for various finite values of N. Example curves are presented in Fig. 2(a). The shape of the curves is typical of simple liquids [15,81,82], with just a few peaks that rapidly diminish in height as k is increased. The first peak of $S(k, N)$ exhibits a finite-size effect of tens of percent, as seen in Fig. 2(a).

At small k, the finite-size effect is more substantial than for the first peak. Instead of tens of percent, $S(k, N)$ changes by much more than a factor of 2 as N is varied, as seen in Fig. 2(b), where we have magnified the low-k portion of the curves.

Since we are especially interested in the static structure factor at $k = 0$, we will extrapolate $S(k, N)$ to $k \to 0$. This extrapolation is done by fitting $S(k, N)$ data points to a parabola,

$$S(k, N) = S(0, N) + Ak^2, \tag{13}$$

as in the work of Huang *et al.* [83]. We note that the fit coefficient A may depend on temperature and the nature of the physical system. More importantly for our analysis, the intercept $S(0, N)$ is the desired estimate, for a finite N. Because Eq. (13) fits our simulation data well in Fig. 2(b), for $ka \leqslant 1$, we will use the parabola of Huang *et al.* to estimate $S(0, N)$.

We note that our simulation data for $S(k, N)$ vary monotonically with k, as can be seen in Fig. 2(b). However, there are other physical systems where the static structure factor is not monotonic with k so that Eq. (13) could not be used directly. In some physical systems [36,83–89], the static structure factor exhibits an upturn feature at small k, where the static structure factor increases instead of decreases at the smallest values of k. Huang *et al.* called such a feather an enhancement and they found that for water they could generalize Eq. (13) by adding an anomalous term, in the fit to the static structure factor data

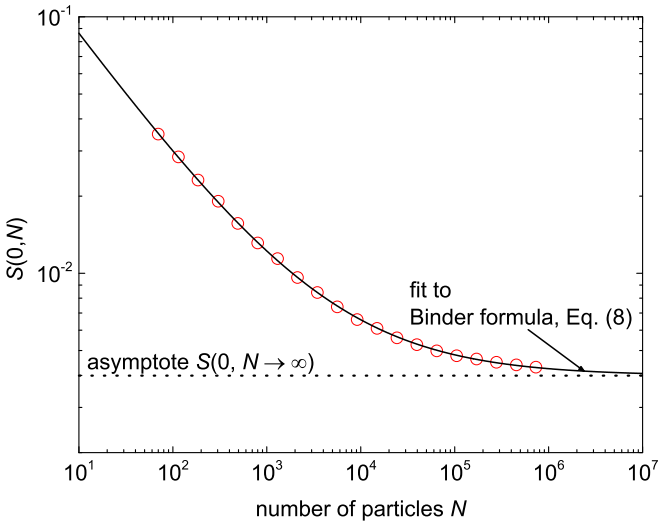

FIG. 3. Finite-size dependence of $S(0, N)$. We found that $S(0, N)$ can vary by an order of magnitude, as N is varied from 70 to 736 771. The $S(0, N)$ data points shown here were obtained as in Fig. 2(b); their error bars are smaller than the symbol size. The solid line is a fit to the Binder formula (8), which has two free parameters: the asymptotic value $S(0, N \to \infty)$ and a coefficient b. For our 2D Yukawa liquid at $T = 1.19T_m$, we obtained $S(0, N \to \infty) = 3.99 \times 10^{-3}$ as our estimate of $S(0)$ for an infinite system, while the coefficient b was found to be 0.260. The good fit gives us confidence that the Binder formula is useful for this 2D liquid.

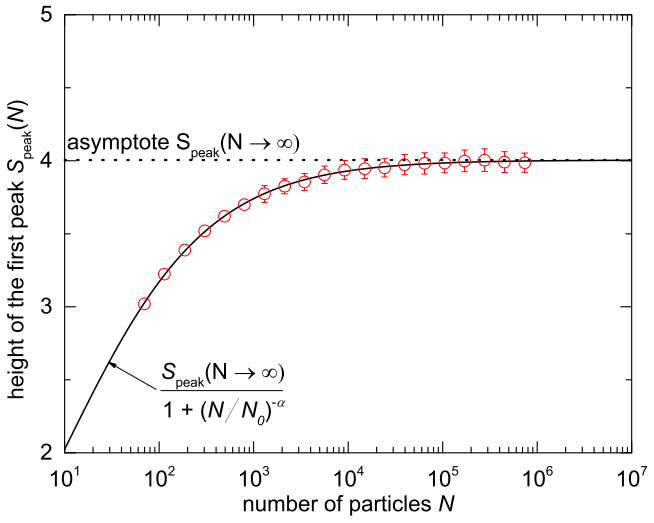

FIG. 4. Finite-size dependence of the height of the first peak of $S(k, N)$. The data points were obtained by a quadratic fit at the first peak. The solid line is the fit to Eq. (11), which has three free parameters, an exponent α, an asymptotic value $S_{\rm peak} \equiv S_{\rm peak}(N \to \infty)$, and a coefficient N_0. The exponent and the coefficient were found to be 0.57 and 9.6, respectively, while the asymptotic value, i.e., $S_{\rm peak}$ for an infinite system, was found to be 4.0 for our simulated liquid. The error bars are shown where they are bigger than the symbol size. These error bars, as well as the scatter in the data points, became bigger at large N due to random errors that arose from the quadratic fit to a first peak that became narrower and therefore more difficult to fit at large N.

points. For such a physical system, that generalized fitting scheme would still allow obtaining $S(0, N)$.

Finite-size effects for $S(0, N)$, which are noticeable even over a limited range of N in Fig. 2(b), are even more profound over a wider range of N, as we show in Fig. 3. In particular, $S(0, N)$ is reduced by nearly an order of magnitude over the wide range of N.

Finite-size effects for the height of the first peak $S_{\rm peak}(N)$ are weaker than those for $S(0, N)$, as shown in Fig. 4. There is at most 25% reduction in $S_{\rm peak}(N)$ over the range of N that we investigated. Since the peak height has this weak dependence on N, we needed to obtain the values of $S_{\rm peak}(N)$ in Fig. 4 with good practical precision. We do this by using a quadratic fit of several data points of $S(k, N)$ near its first peak.

B. Formulas for finite-size effects

1. $S(k, N)$ at small k

We used our simulation data to test the Binder formula (8) for the finite-size effect for $S(0, N)$. This test is shown in Fig. 3. With two free parameters, we find that it is possible for the Binder formula to fit the simulation data very well. The difference between the individual data points and the fit was only 0.56%, on average.

Having found that the Binder formula fits the data well, we can exploit the fit parameter that has a special physical significance, the asymptotic value $S(0, N \to \infty)$. We found this value to be 3.99×10^{-3} for our 2D Yukawa liquid at the simulated temperature. This asymptotic value serves as our best estimate for $S(0)$ for an infinite system.

Another use of the asymptotic value $S(0, N \to \infty)$ is quantifying the finite-size effect for the static structure factor at $k = 0$. We define a discrepancy as the percentage difference between a data point $S(0, N)$ and the asymptotic value $S(0, N \to \infty)$. This discrepancy

$$[S(0, N) - S(0, N \to \infty)]/S(0, N \to \infty) \qquad (14)$$

is plotted in Fig. 5, where we see that it can be very large, unless N is closer to 1×10^6 than to 1000 for this 2D system. Moreover, the discrepancy diminishes rather slowly with N, with a $-1/2$ power-law scaling found in Fig. 5, as one would expect from examining the Binder formula (8).

We note that there would be an even more unfavorable $-1/3$ power law for a 3D system. Thus, a large simulation would be required to obtain a reasonable estimate of $S(0)$, for a simulation of 3D system using a single value of N. To improve upon this situation, one could exploit the Binder formula as an extrapolation, as we suggest later.

Since the asymptote $S(0, N \to \infty)$ is a particularly useful result from fitting to the Binder formula, we investigated whether there is an alternative formula that would offer a further improvement in obtaining the value of this asymptote. In our literature search for the isothermal compressibility, we found that there is a lesser-known formula that extends the Binder formula by adding a higher-order expansion term. This formula, which was proposed by Rovere *et al.* [3] for isothermal compressibility, can be rewritten for static structure factor of a 2D system, as

$$S(0, N) = S(0) + bN^{-1/2} + cN^{-1}, \qquad (15)$$

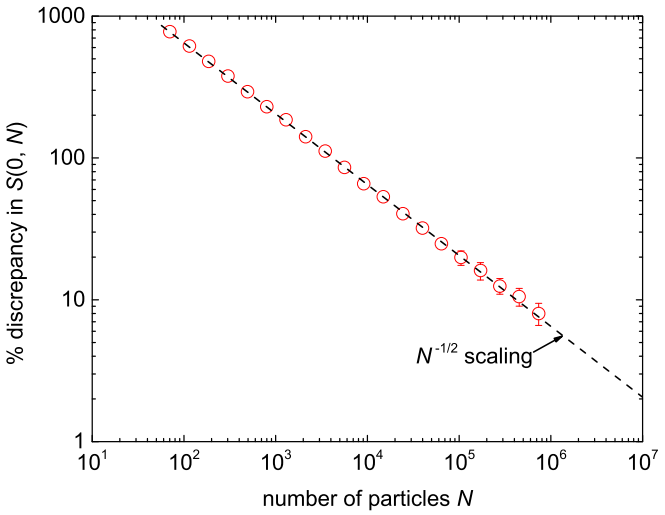

FIG. 5. Percent discrepancy in $S(0, N)$. Data points were obtained by using Eq. (14), which simply defines the discrepancy as the difference $S(0, N) - S(0, N \to \infty)$, obtained from Fig. 3, normalized by the asymptotic value $S(0, N \to \infty)$. The error bars, obtained by propagation of errors, are shown only if they are bigger than the symbol size. The dashed line that we drew through our data points has a slope corresponding to the power law predicted for two dimensions by the Binder formula, $N^{-1/2}$. For three dimensions we would expect a weaker scaling of $N^{-1/3}$, which might therefore require a larger simulation than for our 2D liquid.

which has three fit parameters instead of two. We tested this Rovere formula by fitting to our simulation data and found that the difference between the individual data points and the fit was only 0.62% on average, which is comparable to the 0.56% difference for the Binder formula. The asymptote $S(0) \equiv S(0, N \to \infty)$, which is one of the fit parameters, was 3.96×10^{-3} for our 2D simulation data. This asymptote differs from that of the Binder formula by less than 1%, so we judge, for our 2D system, that there is no great advantage in the additional complexity of the Rovere formula.

2. *Height of the first peak of S(k, N)*

Another result is the finite-size effect for $S_{\text{peak}}(N)$ in Fig. 4. We tested our empirical formula (11) by fitting to our simulation data. There is good agreement between the fit and the data, as seen in Fig. 4. We found only a 0.17% difference, on average, between the individual data points and the fit.

From the fit to Eq. (11), one can obtain the asymptotic value $S_{\text{peak}}(N \to \infty)$. This value serves as our best estimate of S_{peak} for an infinite system. The asymptotic value was found to be 4.0 for our 2D Yukawa liquid.

To quantify the finite-size effect for $S_{\text{peak}}(N)$, we can define a discrepancy similar to the one for $S(0, N)$. This percent discrepancy is defined as

$$[S_{\text{peak}}(N) - S_{\text{peak}}(N \to \infty)]/S_{\text{peak}}(N \to \infty), \qquad (16)$$

which is plotted in Fig. 6. It can be seen from the figure that the finite-size effect for $S_{\text{peak}}(N)$ is at most a 25% effect.

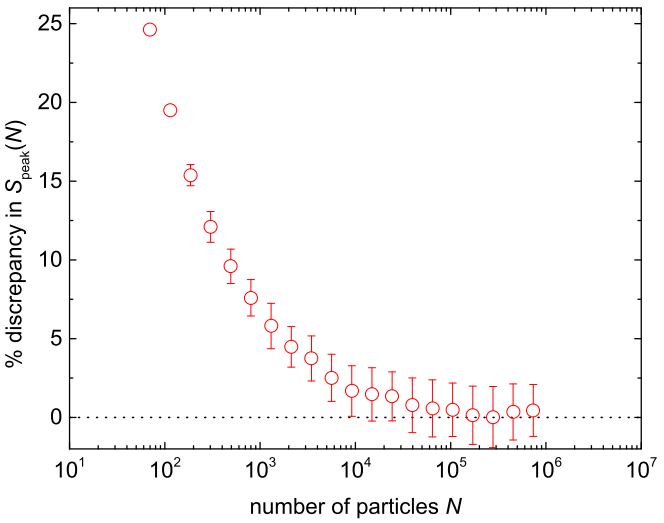

FIG. 6. Percent discrepancy in $S_{\text{peak}}(N)$. The discrepancy was obtained by using Eq. (16), with an input of the data points $S_{\text{peak}}(N)$ and the asymptotic value $S_{\text{peak}}(N \to \infty)$ from Fig. 4. The dotted line indicates 0% discrepancy. The error bars, obtained by propagation of error, are bigger at large N for the same reason as in Fig. 4.

3. *Hyperuniformity index H*

We now quantify the finite-size effect for the hyperuniformity index H for our 2D Yukawa liquid. We obtained the hyperuniformity index $H(N) \equiv S(0, N)/S_{\text{peak}}(N)$ over the same range of N that was investigated. The result is shown in Fig. 7.

As a practical approach of estimating H, corrected for finite-size effects, we simply divide our two asymptotic values $S(0, N \to \infty)$ and $S_{\text{peak}}(N \to \infty)$ that were obtained

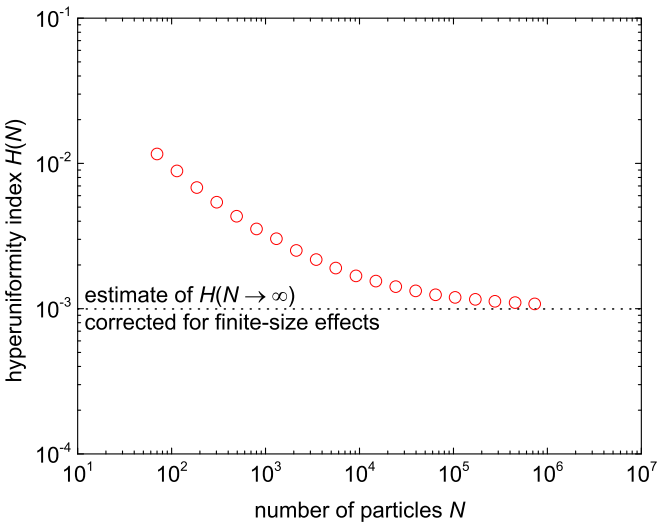

FIG. 7. Finite-size dependence of the hyperuniformity index H. Each data point was calculated as $S(0, N)/S_{\text{peak}}(N)$. The error bars are smaller than the symbol size. The dotted line is the result of the quotient of asymptotic values $S(0, N \to \infty)/S_{\text{peak}}(N \to \infty) = 1.0 \times 10^{-3}$, which were obtained from Figs. 3 and 4. This quotient is our best estimate of the hyperuniformity index for an infinite system $H(N \to \infty)$.

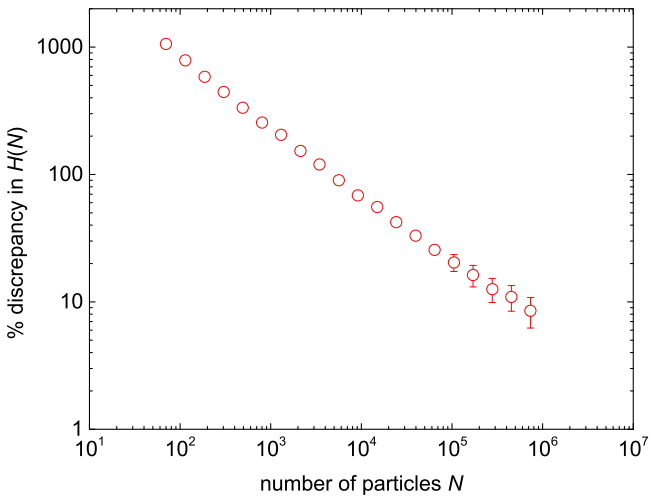

FIG. 8. Percent discrepancy in $H(N)$ obtained from Eq. (17). The inputs to the calculation of this discrepancy were the data points $H(N)$ and our estimate of $H(N \to \infty)$ from Fig. 7. This result is for a 2D Yukawa liquid; we expect that the percent discrepancy would diminish more weakly with N for a 3D system. Only those error bars that are larger than the symbol size are shown.

by fitting to the Binder formula and our empirical formula, respectively. The result, which is our estimate of the hyperuniformity index for an infinite system, is $H \equiv H(N \to \infty) = 1.0 \times 10^{-3}$.

We can also quantify the finite-size effect for $H(N)$. This can done as above by defining the percent discrepancy

$$[H(N) - H(N \to \infty)]/H(N \to \infty). \tag{17}$$

This discrepancy is plotted in Fig. 8, where we see about the same percent discrepancy as for $S(0, N)$ in Fig. 5.

VI. SUGGESTED PROCEDURES FOR CORRECTING $S(k)$ DATA TO OBTAIN $S(0)$ AND S_{peak}

We now suggest procedures to obtain $S(0)$, S_{peak}, and the hyperuniformity index H, all corrected for finite-size effects. These procedures start with $S(k, N)$ curves that were obtained from particle-position data, from either simulation or experiment.

To obtain $S(0)$, corrected for finite-size effects, there are two steps. The first step yields $S(0, N)$, which is an input to the second step that yields $S(0)$.

The first step in finding $S(0)$ starts with the $S(k, N)$ curve for a given value of N. One then fits that curve to an appropriate expression. The expression we used was the parabola of Eq. (13), since there was no upturn in our $S(k, N)$ data at small k. This fitting will yield $S(0, N)$, as one of the fit parameters. This is essentially the asymptotic value at small k. For an experiment or simulation which, unlike ours, has a static structure factor with an upturn at small k, the fitting formula can be modified by adding a term to Eq. (13), for example, the term in Eq. (2) of Ref. [83].

The second step is to use $S(0, N)$, from the first step, as an input to the Binder formula. This formula is Eq. (10) or (9), for two or three dimensions, respectively. If the coefficient b is already known for a given substance and temperature, this can be done with $S(0, N)$ for just a single value of N. Otherwise, one must use $S(0, N)$ data for multiple values of N and fit to the Binder formula to obtain that coefficient, as we did in Sec. V. The result of using the Binder formula is the asymptotic value $S(0, N \to \infty)$, which is the same as the desired quantity $S(0)$, corrected for finite-size effects.

To obtain S_{peak}, we use our empirical formula (12). The input for this formula is the height of that peak, for multiple values of N, i.e., $S_{\text{peak}}(N)$. The result of this step is the asymptotic value $S_{\text{peak}}(N \to \infty)$, which is the same as the desired quantity S_{peak}, the height of the first peak corrected for finite-size effects. An artifact of small N is that the first peak tends to be lower and broader than for large N. This tendency has the counterintuitive consequence that error bars for the height of the first peak are bigger for large N, due to random errors arising from quadratic fitting to a narrow peak.

The hyperuniformity index can then be obtained simply by using Eq. (2). For example, for our 2D Yukawa liquid simulation data, we obtained $H \equiv S(0)/S_{\text{peak}} = 1.0 \times 10^{-3}$. This value is lower than the estimate 3.7×10^{-3} that was reported by Zhuravlyov *et al.* [42] for a simulation with $N = 791$, without correcting for finite-size effects. We note that lower values of H indicate a condition closer to hyperuniformity and that some authors consider the value of 1.0×10^{-3} attained in our simulation to be the threshold for effective hyperuniformity [20,21,24,90].

VII. SUMMARY

We have identified two finite-size effects for the static structure factor: at small k and at the first peak of $S(k, N)$. We have shown that the finite-size effect for $S(k, N)$ at small k can be quite significant, up to an order of magnitude, while the finite-size effect for the height of the first peak is weaker.

To model the finite-size effect for $S(k, N)$ at small k, one can use the Binder formula, which was originally intended for the finite-size effect for isothermal compressibility. The Binder formula expresses $S(0)$ for an infinite system as compared to that for a system of finite size N as a simple difference which scales as a power law of N. That power law, for the correction, is $N^{-1/2}$ or $N^{-1/3}$, for 2D or 3D systems, respectively.

Modeling the finite-size effect for the height of the first peak $S_{\text{peak}}(N)$ required that we devise our own formula, as we found none in the literature. This empirical expression (11) has a correction factor that asymptotically approaches unity.

We identified two challenges arising from finite-size effects that might be unfamiliar to researchers who obtain values S_{peak} and $S(0)$, for example, in calculating the hyperuniformity index. For S_{peak}, we encountered a counterintuitive tendency that the uncertainty in S_{peak} increased, instead of decreased, with larger N, due to the practical issue of measuring the height of a peak that narrows at large N. For $S(0)$, there is a very slow convergence in this value as N is increased, especially in three dimensions where the finite-size correction scales very weakly as $N^{-1/3}$. This problem means that calculating $S(0)$ from the positions of a finite number of particles can have a substantial error, even if the number of particles might seem rather large. To correct $S(0)$ for this finite-size effect, we devised the second step of our two-step procedure.

In the common scenario that one has particle-position data from a simulation or an imaging experiment, the static structure factor curve obtained from those data will be limited by a finite value of N. One might wish to correct those data, especially for $S(0)$ and S_{peak}, to obtain a best estimate of their values for an infinite system. For that purpose, we proposed a two-step correction procedure. The first step, applicable only to $S(0)$, is an extrapolation of the $S(k, N)$ data to $k \to 0$. This extrapolation must be repeated for various values of finite N, to obtain the coefficient b in the Binder formula for the given substance and temperature. The second step is an extrapolation using the Binder formula for $S(0)$ and our empirical formula for S_{peak}.

We tested this two-step procedure using particle-position data from a 2D molecular-dynamics simulation. This simulation had 937 501 particles, allowing us to repeat our analysis of $S(k, N)$ for analyzed regions containing various numbers N of particles. Our simulation was for a liquid with the Yukawa potential, which is a soft potential that models dusty plasmas, among other physical systems. The temperature was above the melting point by a factor of 1.19. For this liquid, we calculated the static structure factor curve for various values of N. The extrapolation to $k \to 0$ in the first step was done by fitting to the parabola of Eq. (13). For the second step, we found that our data for various N closely fit the Binder formula for $S(0)$ and our empirical formula for S_{peak}, yielding values 3.99×10^{-3} and 4.0, respectively. Calculating their ratio, which is the hyperuniformity index $H \equiv S(0)/S_{\text{peak}}$, we found for our 2D Yukawa liquid that $H = 1.0 \times 10^{-3}$, which has been corrected for finite-size effects using our two-step procedure.

We have so far demonstrated our suggested procedure for only one set of parameters. We can suggest that further tests would be useful for different temperatures, densities, interparticle potentials, and three dimensions. Those parameters would affect the value of the coefficient b, as we noted in Sec. II.

In addition to obtaining values of $S(0)$, S_{peak}, and H by considering finite-size effects, our approach can be extended to other material parameters as well. Obviously, this approach will be useful for isothermal compressibility, because of Eq. (1). Other physical quantities that have been identified as being subject to finite-size effects, when they are estimated from simulation data, include the self-diffusion coefficient [91,92], chemical potential [93–95], and molar enthalpy [96]. We expect that the finite-size correction for such quantities might be obtained by our approach provided they have an asymptotic behavior with respect to N, analogous to the Binder formula for $S(0)$ or our empirical formula for S_{peak}.

We note that another material description is the pair correlation function $g(r)$, which like $S(k)$ would have a size dependence when obtained from an analysis of particle-position data. The size dependence for $g(r)$ in this limit was studied theoretically [97] and it was determined that it has a correction proportional to $1/N$. Another correction has also been proposed [Eq. (2) of Ref. [98]], for mixtures of methanol with either water or acetone.

ACKNOWLEDGMENTS

Work at Iowa and Michigan was supported by the Army Research Office under MURI Grant No. W911NF-18-1-0240. Work at Iowa was also supported by the U.S. Department of Energy Grant No. DE-SC0014566 and NASA-JPL Subcontracts No. 1573629, No. 1663801, No. 1672641, and No. 1689926. We thank Jack F. Douglas and our MURI team for helpful discussions.

[1] K. Binder, Z. Phys. B **43**, 119 (1981).
[2] K. Kaski, K. Binder, and J. D. Gunton, Phys. Rev. B **29**, 3996 (1984).
[3] M. Rovere, D. W. Hermann, and K. Binder, Europhys. Lett. **6**, 585 (1988).
[4] M. Rovere, D. W. Heermann, and K. Binder, J. Phys.: Condens. Matter **2**, 7009 (1990).
[5] D. Marx, P. Nielaba, and K. Binder, Phys. Rev. Lett. **67**, 3124 (1991).
[6] M. Rovere, P. Nielaba, and K. Binder, Z. Phys. B **90**, 215 (1993).
[7] S. Sengupta, D. Marx, P. Nielaba, and K. Binder, Phys. Rev. E **49**, 1468 (1994).
[8] D. Marx, P. Nielaba, and K. Binder, Phys. Rev. B **47**, 7788 (1993).
[9] J. Baschnagel and K. Binder, Physica A **204**, 47 (1994).
[10] H. Weber and D. Marx, Europhys. Lett. **27**, 593 (1994).
[11] H. Weber, D. Marx, and K. Binder, Phys. Rev. B **51**, 14636 (1995).
[12] C. Borgs and R. Kotecký, J. Stat. Phys. **79**, 43 (1995).
[13] J. J. Salacuse, A. R. Denton, and P. A. Egelstaff, Phys. Rev. E **53**, 2382 (1996).
[14] F. L. Román, J. A. White, and S. Velasco, J. Chem. Phys. **107**, 4635 (1997).
[15] J.-P. Hansen and I. R. McDonald, *Theory of Simple Liquids* (Elsevier, New York, 1986).
[16] J.-P. Boon and S. Yip, *Molecular Hydrodynamics* (Dover, New York, 1991).
[17] U. Balucani and M. Zoppi, *Dynamics of the Liquid State* (Oxford University Press, New York, 1994).
[18] S. Torquato and F. H. Stillinger, Phys. Rev. E **68**, 041113 (2003).
[19] G. Zhang, F. H. Stillinger, and S. Torquato, Sci. Rep. **6**, 36963 (2016).
[20] A. Chremos and J. F. Douglas, Ann. Phys. (NY) **529**, 1600342 (2017).
[21] F. Martelli, S. Torquato, N. Giovambattista, and R. Car, Phys. Rev. Lett. **119**, 136002 (2017).
[22] S. Torquato, Phys. Rep. **745**, 1 (2018).
[23] D. Chen, E. Lomba, and S. Torquato, Phys. Chem. Chem. Phys. **20**, 17557 (2018).
[24] A. Chremos and J. F. Douglas, Phys. Rev. Lett. **121**, 258002 (2018).
[25] G. Rumi, J. Aragón Sánchez, F. Elías, R. Cortés Maldonado, J. Puig, N. R. Cejas Bolecek, G. Nieva, M. Konczykowski, Y. Fasano, and A. B. Kolton, Phys. Rev. Res. **1**, 033057 (2019).
[26] G. Zhang and S. Torquato, Phys. Rev. E **101**, 032124 (2020).
[27] A. Chremos, J. Chem. Phys. **153**, 054902 (2020).

[28] Z. Ma, E. Lomba, and S. Torquato, Phys. Rev. Lett. **125**, 068002 (2020).

[29] D. Chen, Y. Zheng, L. Liu, G. Zhang, M. Chen, Y. Jiao, and H. Zhuang, Proc. Natl. Acad. Sci. USA **118**, e2016862118 (2021).

[30] S. Mitra, A. D. S. Parmar, P. Leishangthem, S. Sastry, and G. Foffi, J. Stat. Mech. (2021) 033203.

[31] S. Torquato, Phys. Rev. E **103**, 052126 (2021).

[32] D. Chen, Y. Zheng, C.-H. Lee, S. Kang, W. Zhu, H. Zhuang, P. Y. Huang, and Y. Jiao, Phys. Rev. B **103**, 224102 (2021).

[33] Ü. S. Nizam, G. Makey, M. Barbier, S. S. Kahraman, E. Demir, E. E. Shafigh, S. Galioglu, D. Vahabli, S. Hüsnügil, M. H. Güneş, E. Yelesti, and S. Ilday, J. Phys.: Condens. Matter **33**, 304002 (2021).

[34] S. Atkinson, G. Zhang, A. B. Hopkins, and S. Torquato, Phys. Rev. E **94**, 012902 (2016).

[35] R. A. Quinn, C. Cui, J. Goree, J. B. Pieper, H. Thomas, and G. E. Morfill, Phys. Rev. E **53**, R2049 (1996).

[36] R. Kurita and E. R. Weeks, Phys. Rev. E **82**, 011403 (2010).

[37] S. Wilken, R. E. Guerra, D. J. Pine, and P. M. Chaikin, Phys. Rev. Lett. **125**, 148001 (2020).

[38] J.-P. Hansen, Phys. Rev. A **8**, 3096 (1973).

[39] C. Aust, M. Kröger, and S. Hess, Macromolecules **32**, 5660 (1999).

[40] J. Horbach and W. Kob, Phys. Rev. B **60**, 3169 (1999).

[41] S. M. Urahata and M. C. C. Ribeiro, J. Chem. Phys. **120**, 1855 (2004).

[42] V. Zhuravlyov, J. Goree, J. F. Douglas, P. Elvati, and A. Violi, Phys. Rev. E **106**, 055212 (2022).

[43] M. E. Fisher and M. N. Barber, Phys. Rev. Lett. **28**, 1516 (1972).

[44] D. P. Landau, Phys. Rev. B **14**, 255 (1976).

[45] F. L. Román, J. A. White, and S. Velasco, Europhys. Lett. **42**, 371 (1998).

[46] P. Shukla and A. Mamun, *Introduction to Dusty Plasma Physics* (Institute of Physics, Bristol, 2001).

[47] P. M. Bellan, *Fundamentals of Plasma Physics* (Cambridge University Press, New York, 2006), Chap. 17.

[48] M. Bonitz, C. Henning, and D. Block, Rep. Prog. Phys. **73**, 066501 (2010).

[49] A. Melzer, *Physics of Dusty Plasmas: An Introduction* (Springer Nature, Cham, 2019).

[50] J. H. Chu and L. I, Phys. Rev. Lett. **72**, 4009 (1994).

[51] R. L. Merlino and J. A. Goree, Phys. Today **57** (7), 32 (2004).

[52] V. E. Fortov, A. V. Ivlev, S. A. Khrapak, A. G. Khrapak, and G. E. Morfill, Phys. Rep. **421**, 1 (2005).

[53] U. Konopka, G. E. Morfill, and L. Ratke, Phys. Rev. Lett. **84**, 891 (2000).

[54] A. A. Sickafoose, J. E. Colwell, M. Horányi, and S. Robertson, J. Geophys. Res. **107**, 1408 (2002).

[55] N. K. Bastykova, A. Z. Kovács, I. Korolov, S. K. Kodanova, T. S. Ramazanov, P. Hartmann, and Z. Donkó, Contrib. Plasma Phys. **55**, 671 (2015).

[56] A. Kananovich and J. Goree, Phys. Rev. E **101**, 043211 (2020).

[57] S. Nunomura, J. Goree, S. Hu, X. Wang, and A. Bhattacharjee, Phys. Rev. E **65**, 066402 (2002).

[58] Z. Donkó, P. Hartmann, and J. Goree, Mod. Phys. Lett. B **21**, 1357 (2007).

[59] Y. Feng, J. Goree, and B. Liu, Phys. Rev. Lett. **105**, 025002 (2010).

[60] J. K. Meyer, I. Laut, S. K. Zhdanov, V. Nosenko, and H. M. Thomas, Phys. Rev. Lett. **119**, 255001 (2017).

[61] N. P. Kryuchkov, E. V. Yakovlev, E. A. Gorbunov, L. Couëdel, A. M. Lipaev, and S. O. Yurchenko, Phys. Rev. Lett. **121**, 075003 (2018).

[62] F. Wieben and D. Block, Phys. Rev. Lett. **123**, 225001 (2019).

[63] N. Chaubey and J. Goree, Front. Phys. **10**, 879092 (2022).

[64] N. Chaubey and J. Goree, J. Phys. D **56**, 375202 (2023).

[65] Y. Feng, J. Goree, and B. Liu, Rev. Sci. Instrum. **78**, 053704 (2007).

[66] S. Ichimaru, Rev. Mod. Phys. **54**, 1017 (1982).

[67] M. S. Murillo, Phys. Plasmas **11**, 2964 (2004).

[68] H. Thomas, G. E. Morfill, V. Demmel, J. Goree, B. Feuerbacher, and D. Möhlmann, Phys. Rev. Lett. **73**, 652 (1994).

[69] Y. Hayashi and K. Tachibana, Jpn. J. Appl. Phys. **33**, L804 (1994).

[70] N. Chaubey, J. Goree, S. J. Lanham, and M. J. Kushner, Phys. Plasmas **28**, 103702 (2021).

[71] N. Chaubey and J. Goree, Phys. Plasmas **29**, 113705 (2022).

[72] M. Wolter and A. Melzer, Phys. Rev. E **71**, 036414 (2005).

[73] V. Nosenko, J. Goree, and A. Piel, Phys. Plasmas **13**, 032106 (2006).

[74] Z. Haralson and J. Goree, IEEE Trans. Plasma Sci. **44**, 549 (2015).

[75] Z. Haralson and J. Goree, Phys. Plasmas **23**, 093703 (2016).

[76] Z. Haralson and J. Goree, Phys. Rev. Lett. **118**, 195001 (2017).

[77] S. Plimpton, J. Comput. Phys. **117**, 1 (1995).

[78] P. Hartmann, G. J. Kalman, Z. Donkó, and K. Kutasi, Phys. Rev. E **72**, 026409 (2005).

[79] G. Bussi, D. Donadio, and M. Parrinello, J. Chem. Phys. **126**, 014101 (2007).

[80] V. Zhuravlyov, J. Goree, P. Elvati, and A. Violi, Static structure factor data for a 2D Yukawa liquid, Iowa Research Online, https://doi.org/10.25820/data.006673.

[81] D. M. North, J. E. Enderby, and P. A. Egelstaff, J. Phys. C **1**, 1075 (1968).

[82] S. Takeda, M. Inui, S. Tamaki, K. Maruyama, and Y. Waseda, J. Phys. Soc. Jpn. **63**, 1794 (1994).

[83] C. Huang, K. T. Wikfeldt, T. Tokushima, D. Nordlund, Y. Harada, U. Bergmann, M. Niebuhr, T. M. Weiss, Y. Horikawa, M. Leetmaa, M. P. Ljungberg, O. Takahashi, A. Lenz, L. Ojamäe, A. P. Lyubartsev, S. Shin, L. G. M. Pettersson, and A. Nilsson, Proc. Natl. Acad. Sci. USA **106**, 15214 (2009).

[84] E. C. Svensson, V. F. Sears, A. D. B. Woods, and P. Martel, Phys. Rev. B **21**, 3638 (1980).

[85] W. Montfrooij, L. A. de Graaf, P. J. Van Den Bosch, A. K. Soper, and W. S. Howells, J. Phys.: Condens. Matter **3**, 4089 (1991).

[86] F. Barocchi, P. Chieux, R. Magli, L. Reatto, and M. Tau, J. Phys.: Condens. Matter **5**, 4299 (1993).

[87] E. W. Fischer, Physica A **201**, 183 (1993).

[88] N. Xu and E. S. C. Ching, Soft Matter **6**, 2944 (2010).

[89] R. Xie, G. G. Long, S. J. Weigand, S. C. Moss, T. Carvalho, S. Roorda, M. Hejna, S. Torquato, and P. J. Steinhardt, Proc. Natl. Acad. Sci. USA **110**, 13250 (2013).

[90] H. Zhang, X. Wang, J. Zhang, H.-B. Yu, and J. F. Douglas, Eur. Phys. J. E **46**, 50 (2023).

[91] S. H. Jamali, R. Hartkamp, C. Bardas, J. Soöhl, T. J. H. Vlugt, and O. A. Moultos, J. Chem. Theory Comput. **14**, 5959 (2018).
[92] A. T. Celebi, S. H. Jamali, A. Bardow, T. J. H. Vlugt, and O. A. Moultos, Mol. Simul. **47**, 831 (2021).
[93] J. I. Siepmann, I. R. McDonald, and D. Frenkel, J. Phys.: Condens. Matter **4**, 679 (1992).
[94] C. M. Herdman, A. Rommal, and A. Del Maestro, Phys. Rev. B **89**, 224502 (2014).
[95] J. P. Thompson and I. C. Sanchez, J. Chem. Phys. **145**, 214103 (2016).
[96] S. K. Schnell, T. J. H. Vlugt, J.-M. Simon, D. Bedeaux, and S. Kjelstrup, Chem. Phys. Lett. **504**, 199 (2011).
[97] J. L. Lebowitz and J. K. Percus, Phys. Rev. **122**, 1675 (1961).
[98] A. Perera, L. Zoranić, F. Sokolić, and R. Mazighi, J. Mol. Liq. **159**, 52 (2011).